SAND2024-00802J

Modeling Geologic Waste Repository Systems Below Residual Saturation

Matthew J. Paul,[a]* Heeho D. Park,[b] Michael Nole,[b] and Scott L. Painter[c]

[a]*Sandia National Laboratories, Nuclear Waste Disposal Research and Analysis, Albuquerque, NM*

[b]*Sandia National Laboratories, Applied Systems Analysis and Research, Albuquerque, NM*

[c]*Oak Ridge National Laboratory, Watershed Systems Modeling, Oak Ridge, TN*

*E-mail: matpaul@sandia.gov

Modeling Geologic Waste Repository Systems Below Residual Saturation

The heat generated by high-level radioactive waste can pose numerical and physical challenges to subsurface flow and transport simulators if the liquid water content in a region near the waste package approaches residual saturation due to evaporation. Here, residual saturation is the fraction of the pore space occupied by liquid water when the hydraulic connectivity through a porous medium is lost, preventing the flow of liquid water. While conventional capillary pressure models represent residual saturation using asymptotically large values of capillary pressure, here residual saturation is effectively modeled as a tortuosity effect alone. Treating the residual fluid as primarily dead-end pores and adsorbed films, relative permeability is independent of capillary pressure below residual saturation. To test this approach, PFLOTRAN is then used to simulate thermal-hydrological conditions resulting from direct disposal of a dual-purpose canister in unsaturated alluvium using both conventional asymptotic and the revised, smooth models. While the two models have comparable results over 100,000 years, the number of flow steps required is reduced by approximately 94%.

Keywords: Capillary Pressure; Matric Potential; Relative Permeability; Residual Saturation

I. Introduction

Unsaturated alluvium is one of several generic deep geologic disposal environments considered in the United States Department of Energy's Spent Fuel and Waste Science Campaign. However, there are physical and numerical challenges associated with modeling fluid flow and heat transport in unsaturated geologic repository systems. One such challenge involves heat released from the radioactive decay of spent nuclear fuel packages, which may significantly elevate temperatures in the host medium of a repository system, resulting in complex thermal-hydrological interactions[1,2]. Thus, simulations of spent fuel and high-level waste repository systems must adequately model coupled thermo-hydrologic interactions in multiphase systems and allow for the

possibility of complete loss of the water phase in regions of elevated temperatures.

In an isothermal system, a partially saturated porous medium will drain until the water saturation index reaches a small but non-zero value known as the residual saturation. Here saturation index refers to the fraction of the pore space that is filled with liquid water. Many models, such as the van Genuchten[3] model, represent the cut-off of drainage behavior by allowing the capillary pressure to approach an infinite value at some small but non-zero residual saturation. As a result, when relative permeability is modeled as being proportional to the inverse of capillary pressure, as in the Mualem[4] model, the relative permeability approaches zero as water content approaches residual saturation. Consequently, the water saturation index can never fall below the residual limit by liquid-phase flow alone.

However, water can be removed below the residual saturation by evaporation and miscible gas-phase flow. This can be encountered in high-level nuclear waste repositories as the decay heat increases the temperature, driving evaporation and convection. Such a scenario was simulated by *in situ* heater tests at the Exploratory Studies Facility at Yucca Mountain[5] and has been projected to occur in repositories sited in tuff[1] and shale[2]. As capillary pressure cannot be infinite, either physically or numerically, when water is driven off past the residual saturation, several extensions have been recently implemented in PFLOTRAN as part of the Geological Disposal Safety Assessment (GDSA) development project[6]. However, these extensions can introduce their own physical or numerical idiosyncrasies.

Numerically, the capillary pressure curve must be both continuous and smooth for Newton's method to efficiently solve the implicit system of equations describing mass and heat transfer in multiphase systems. Consequently, smooth extensions to capillary pressure at low water saturation have shown significant improvement in performance on

a series of benchmark problems. One such benchmark problem is presented here whereby evaporation, boiling from the thermal pulse of a waste package, and infiltration from rainfall in an unsaturated alluvium system all interact to dynamically dry and re-wet the system. Using the new smooth capillary pressure extensions, this problem can finish where it had previously stalled due to unacceptably small timesteps necessary for convergence.

II. Background

A broad range of possible scenarios for deep geologic disposal of radioactive waste are being considered under the U.S. Department of Energy's Geologic Disposal Safety Assessment (GDSA) program. Within this generic disposal R&D program, it is particularly challenging to model waste package heating and multiphase flow in the unsaturated zone (UZ) reference case due to the complex interplay of capillary forces, evaporation and even boiling in the porous media. The generic UZ reference case consists of a mined repository in unsaturated alluvium located 255 m below the land surface, and the repository is modeled to contain hot commercial spent nuclear fuel[7]. The water table depth is assumed to be at 500 m depth. Aside from infiltration of rainwater, at 245 m above the water table, the initial water content will initially be near residual saturation (Figure 1).

At the same time, due to radioactive decay heat and limited conductive heat transport away from the waste packages in the subsurface, the temperature in the spent nuclear fuel waste packages will be elevated. Initial calculations have estimated peak temperatures ranging from 150 C to 350 C in the several hundred years post-closure. While the temperature in the surrounding porous media will be less than this peak, the elevated temperatures will drive elevated rates of evaporation or even boiling at ambient

or possibly slightly elevated pressures.

While water is at an elevated temperature near the waste packages, most of the repository system remains near the ambient temperature of 27 C. Consequently, water vapor generated by decay heat will not be removed in a closed repository system. After gas phase transport, the water vapor is anticipated to condense on cooler materials, driving natural convection flows[8].

This situation can be problematic when applying standard approaches to modeling two-phase flow in porous media. For example, the two-phase flow model in PFLOTRAN was initially adopted from using the model described by Chen et al.[9]. The numerical difficulty due to the singularity in the capillary pressure model has previously been addressed in PFLOTRAN[10] using piecewise extensions similar to those described by Sun et al.[11] One intention of this work is to examine how or if the extensions should affect relative permeability models.

III. Theory

A common but ultimately empirical approach is to follow the Muskat-Meres model and extend Darcy's law to two-phase systems by introducing the concept of relative permeabilities.[12] The phenomenon of residual saturation, a low but nevertheless non-zero degree of saturation where the relative permeability becomes zero was immediately recognized. While "irreducible" or "residual" saturation depends upon the process as saturation can be reduced further by evaporation, centrifugation or other processes,[13,14] here, residual saturation is defined as the irreducible saturation under gravity drainage.

Independent of the relative permeability model, Richards[15] modeled the phenomenon of capillary conduction of a wetting fluid in porous media. Specifically, Richards describes

the flow of capillary liquid on surfaces already wetted by an adsorbed film, which is in essence, above residual saturation. Richards explicitly does not consider the flow of adsorbed films that may predominate at very low degrees of saturation[16]. By merging the concepts of relative permeability and capillary pressure the generalized Darcy equations are formulated.[17,18]

Darcian Two-Phase Flow Model.

Here, the two phases of interest are the wetting phase, for this work liquid water denoted with the subscript w, and the non-wetting gas phase, denoted with the subscript g.

$$q_w = -k_i \frac{k_{rw}}{\mu_w} \nabla p_w \tag{1}$$

$$q_g = -k_i \frac{k_{rg}}{\mu_g} \nabla p_g \tag{2}$$

$$p_c = p_g - p_w \tag{3}$$

Here, q_w and q_g are the volumetric fluxes of liquid water and gaseous air, respectively. k_i is the intrinsic permeability while k_{rw} and k_{rg} are the relative permeabilities of the corresponding phases. Finally, μ and p represent the dynamic viscosity and the effective pressure of their respective phases. The volumetric fluxes calculated by Darcy's Law describe the total volumetric flux of the phase. The volumetric flux of individual components is typically found relative to the mean volumetric flux using the advective-diffusive model. For example, gradients in water vapor partial pressure can drive diffusive flow even where there is no total pressure gradient. An advantage of the conventional two-phase Darcian Flow model is its generality. The major disadvantage is that its validity is entirely dependent upon the underlying models for both relative

permeability and capillary pressure.

Modeling the equations becomes numerically challenging as both relative permeability and capillary pressure are expressed as functions of the degree of phase saturation within a given region. While phase saturation can be defined in other ways, here phase saturation will be defined on a fractional volumetric basis such that the sum of the phase saturations equals one. That is, if the only two phases in the pore space are liquid water and gas, the degrees of saturation are complementary and will be denoted as $S_w + S_g = 1$.

As the Darcian flow model is only valid for low Reynolds number creeping flow, i.e., where inertial forces are negligible compared with viscous forces, the volumetric flux is modeled as responding instantly to a change in pressure. This enables direct substitution of the volumetric flux into a mass balance. As this work is focused on the residual saturation of water, only the mass balance for the liquid phase will be discussed here.

$$\phi \frac{\partial(\rho_w S_w)}{\partial t} + \nabla \cdot (\rho_w q_w) = Q_w \tag{4}$$

Here, ρ_w represents the mass density, ϕ the porosity, and Q_w the source/sink term for the liquid phase of water, including evaporation and condensation. In practice, PFLOTRAN does not independently model evaporation and condensation but rather couples the liquid and gas phase flow under assumption of local equilibrium. As the liquid phase is nearly incompressible, the density of the fluid is nearly constant with respect to pressure and water saturation is the primary variable. So long as the simulation remains above residual saturation, where relative permeability and capillary pressure are continuously defined, this model can be solved by ordinary methods. Similarly, below residual saturation, the volumetric flux of the liquid phase is zero. This

simplifies the mass balance, though as the rate of evaporation or condensation is dependent on the degree of water saturation, this too is a non-linear equation.

$$\phi \frac{\partial(\rho_w S_w)}{\partial t} = Q_w \tag{5}$$

A numerical solution either above or below residual saturation is a tractable problem. The numerical difficulty occurs more specifically in the vicinity of the residual saturation. Because the flow of each phase is itself a function of relative permeability, non-wetting pressure, and capillary pressure, each term must be discretized. This however requires that both relative permeability and capillary pressure be continuous and differentiable over the entire domain. This is not the case for many frequently used capillary pressure models, such as Brooks-Corey[19] and van Genuchten[3]. Rather, capillary pressure is permitted to asymptotically approach infinity at some residual degree of saturation. Consequently, the derivative of capillary pressure with respect to saturation is infinite at this asymptote, leading to a $0 \cdot \infty$ singularity in the expression for flow. While analytical methods can readily evaluate this expression to correctly approach zero flow at residual saturation, discrete numerical models may not.

For example, depending upon the discretization of Equation 1, a finite difference of either capillary pressures or saturation can be performed. In the first approach, this requires subtracting two similar but exceedingly large capillary pressures. That is, $\frac{\Delta P_c}{\Delta x} \rightarrow \frac{\infty - \infty}{\Delta x}$. As floating-point expressions have limited precision, the truncation error when finding the difference of extremely large but similar values is very large. In the second approach, the analytical derivative of capillary pressure is utilized, but this nevertheless takes on a very large value that is subsequently multiplied by the numerical difference between two very similar degrees of saturation. That is, $\frac{dP}{dx} \sim \frac{dP}{dS_w} \cdot \frac{\Delta S_w}{\Delta x} \rightarrow \infty \cdot \frac{0-0}{\Delta x}$. In

either case, when the erroneous large pressure gradient is multiplied by the small but non-zero relative permeability, errors in the calculated flow may result.

To mitigate this numerical difficulty, PFLOTRAN previously truncated capillary pressure to a user-assignable fixed capillary pressure maximum. This has the effect of bounding the derivative or differential of capillary pressure to modest values. While this indeed limits flow to finite values and the system of equations is made continuous, it has the unintended secondary effect of introducing a jump discontinuity in the derivative of capillary pressure.

A jump discontinuity in the derivative of capillary pressure is particularly problematic when a Newton solver is utilized. If an iteration crosses a jump discontinuity in the derivative, the derivative immediately jumps from finite but nevertheless large values to a zero value. Due to compressibility, the overall derivative of the mass with respect to saturation is not exactly zero, but it is nevertheless exceedingly small. While Newton's method may slowly converge to a saturation near the junction point, upon crossing the jump discontinuity, the next iteration may predict a vastly different saturation. This can result in Newton's method failing to converge or only converging when the size of the discrete time step is reduced. While this numerical difficulty is specific to Newton's method, and other non-linear solvers now available for use with PFLOTRAN[20] only require continuity and not smoothness, even alternative solvers have been shown to converge more rapidly where the system is both continuous and smooth[10]. Rather than truncating capillary pressure to some flat maximum, a number of continuous and smooth capillary pressure extensions were presented by Sun et al.[11] However, beyond numerical performance, here a physical justification for choice of extension is discussed to justify their use in modelling a waste repository systems below residual saturation.

Residual Saturation, Relative Permeability and Capillary Pressure.

An open question is if or how the relative permeability model should be affected by the introduction of a capillary pressure extension. Sun et al.[11] remap relative permeability only between the junction point and residual saturation. In contrast, Rossi and Nimmo[21] utilize the Mualem model and propose extending relative permeability to oven-dry conditions, essentially eliminating the phenomenon of residual saturation. And lastly, Webb[22] suggests neither is necessary and the original relative permeability expressions are satisfactory, regardless of the extension.

It is unclear if any of these three approaches are consistent with the underlying theories of the Burdine or Mualem relative permeability models. While models based on bundles of tubes in Hagen-Poiseuille flow can be drawn for single-phase flow in porous media, for multi-phase flow, the relative permeability represents the averaging behavior over many discontinuous regions[23]. Furthermore, the two-phase Darcian flow model presumes there is neither entrainment of the liquid phase by the gas or of the gas by the liquid. That is, the two-phase velocities are calculated with respect to the solid phase frame of reference and do not interact with each other. Thus, any relative permeability model should be considered as approximate. Nevertheless, the models of Burdine[24,25] and Mualem[4] have theoretical frameworks even if they require empirical correlations.

In the development of the first model, Burdine *et al*. performed detailed characterizations of petroleum reservoir rocks[24] and later developed a conceptual model for estimating the permeability by summing over the volume, area, and tortuosity of the fluid filled pores[25]. An important aspect of this model is the introduction of an "effective" tortuosity ratio. Let the intrinsic tortuosity T_i be the ratio of pathlength to displacement at full saturation. Similarly, let the wetting phase tortuosity T_w be the ratio

of pathlength to displacement restricted to pathways filled by the wetting phase. The effective tortuosity ratio T_w is then the product of the intrinsic tortuosity and wetting phase tortuosity, which can be expressed as $T_w(S_w) = X_{rw}(S_w)T_i$. Burdine showed empirically that this ratio has a linear relationship between residual and full saturation; that is $X_{rw} = \frac{S_w - S_r}{1 - S_r}$. While Burdine arrived at this fitting tortuosity data, this term was later supplanted by "effective" saturation, a term attributed to Corey[19].

Importantly, tortuosity is a property of the connectivity of the pores in the medium and is not a function of pore radius alone. For example, a dead-end pore or vesicle has an infinite tortuosity, regardless of its radius and contribution to volume. Similar to dead end pores, pores that that have viable pathways at higher degrees of saturation become hydraulically isolated at lower degrees of saturation[14]. For example, if the only hydraulic pathway through a pore requires an adjacent pore of larger radius to be filled, the smaller pore is hydraulically isolated if the adjacent pore is not wetted. Thus, an effective tortuosity of zero must occur at the degree of saturation where any remaining liquid filled pores lack hydraulic connectivity. This logically occurs at some large but nevertheless finite capillary pressure.

In the Burdine model, the effective tortuosity is applied uniformly to all pores, regardless of their intrinsic tortuosity or hydraulic radius. Burdine then expressed the relative permeability as a ratio of the permeability of all pathways to the intrinsic permeability. That is, let $V_{j,w}$ be the fractional volume and $r_{j,w}$ be the hydraulic radius of the wetted pore, and T_j be the intrinsic tortuosity of the pore – regardless of which fluid fills is – the relative permeability of a medium described by such pore distribution data can be expressed as a summation.

$$k_{rw} = \frac{\phi X_{rw}^2}{k_i} \sum_{j=0}^{n} \frac{V_{j,w} r_{j,w}^2}{T_j^2} \tag{6}$$

Unfortunately, detailed pore size and tortuosity data are scarcely available, making estimation of permeability by such summation inconvenient. Instead, it is commonplace for pore size distributions to be inferred from the capillary pressure data and assumptions made about the relative tortuosity. However, in the Brooks-Corey version, all pores are assumed to have not only uniform effective tortuosity but also intrinsic tortuosity. In doing so, the relative permeability can be expressed as the ratio of the mean squared hydraulic radius at partial and full saturation.

$$k_{rw}(S_w) = X_{rw}^2 \frac{S_w \overline{r_w(S_w)^2}}{\overline{r_w^2(1)}} \tag{7}$$

Under these assumptions, the mean squared hydraulic radius at different degrees of saturation can be found using the Young-Laplace equation. Let γ be the surface tension of the fluid and θ be the constant angle for a cylindrical pore. Provided with a capillary pressure model, the hydraulic radius is modeled as a function of saturation.

$$r_w(S_w) = \frac{2\gamma \cos\theta}{P_c(S_w)} \tag{8}$$

Consequently, the mean squared hydraulic radius at with degree of saturation is expressed as an integral of inverse capillary pressure squared.

$$\overline{r_w(S_w)^2} = \frac{4\gamma^2 \cos^2\theta}{S_w} \int_0^{S_w} \frac{dS}{P_c(S)^2} \tag{9}$$

Substituting this expression into the previous equation, the relative permeability becomes the effective tortuosity squared times the ratio of two integrals.

$$k_{rw} = X_{rw}^2 \frac{\int_0^{Sw} \frac{dS'_w}{P_c^2}}{\int_0^1 \frac{dS'_w}{P_c^2}} \tag{10}$$

This expression is, however, problematic as integration is to be conducted over all degrees of saturation, even those where capillary pressure is infinite or ill-defined. While requiring capillary pressure to be infinite or very large allows the area to the left of residual saturation to be neglected, this suggests that residual saturation can only occur at very large capillary pressures, ignoring the existence of isolated pores and adsorbed films.

Understanding that the residual saturation is a property of relative permeability and not capillary pressure opens the model to different representations of capillary pressure below residual saturation. Rather than applying a purely mechanical definition of Darcy's Law, Edlefsen and Anderson developed an expression based on the thermodynamic free energy[26]. Rather than considering only mechanical pressure, gravitational potential, and capillary pressure to drive flow, Darcy's Law is expressed in terms of Gibbs free energy f_w.

$$q_w = - k_i \frac{k_{rw}}{\mu_w} \rho_w \nabla f_w \tag{11}$$

For any process to be spontaneous, the free energy of the system decreases, just as a fluid is modeled to flow from a higher to lower mechanical pressures. The primary difference is in the understanding of the potentials as energy densities rather than mechanical stresses. For the scope of this simulation, the free energy difference between two locations is the sum of contributions from pressure, gravity, and capillary – or more generically – matric potential. Note that it is the external pressure, in this case the gas phase pressure, that is relevant to enthalpy and the Gibbs free energy. The gravitational

potential energy is defined as usual in a uniform gravitational field g. All changes in free energy due to the presence of the matrix are implicitly included in the matric potential ψ_m.

$$df = \frac{dP}{\rho} + g\, dz + d\psi_m \tag{12}$$

The free energy expression applies to both the gas and liquid phases. However, the gas phase is characterized by weak intermolecular interactions, both with itself and with the solid phase. Thereby, the matric potential of the gas phase is assumed to be negligible and any gas-matrix interactions, such as due to vapor adsorption, shall be represented by the liquid phase. This is due in part because the adsorbed water vapor has a density similar to the liquid phase. Thus, in this model, there is no distinction between capillary and adsorbed fluids, but rather the matric potential is the summation of adsorptive and capillary terms, [27,28] or equivalently the short- and long-range intermolecular interactions,[29] at a given degree of saturation. While the matric potential can alter the density of the fluid relative to the bulk liquid reference state[30], in most cases this difference in density compared to the bulk liquid phase is small and can be neglected. Thus, under the presumption of constant density, the matric potential per unit mass is equivalently expressed as a capillary pressure, regardless of if the model is representing capillary liquid or adsorbates.

$$dP_c = -\rho\, d\psi_m \tag{13}$$

Similarly, the free energy gradient of the combined condensate phase is equivalent to the conventional two-phase flow model.

$$\nabla f = \frac{1}{\rho} \nabla\left(P_g + \rho g z - P_c\right) \tag{14}$$

The advantage of this representation is that the capillary pressure can be related to available thermodynamic data. As simulated by Zhang, Dong and Liu[31], the lowest matric potential of water on quartz – or the highest "capillary pressure" – was calculated to be 2.00 GPa. In contrast, in clay-bearing soil samples tested by Campbell and Shiozawa[32], the maximum "capillary pressure" was fitted by both Rossi and Nimmo[21] and Webb[22] to be 1.0 GPa. This is consistent with the measured heat of water desorption from kaolinite, illite, and smectite of 17-18 kJ/mol[33] or, under the assumption of incompressibility, effectively 0.94-1 GPa. While there is limited data between the pure adsorbate and capillary regimes, an exponential capillary pressure extension to a limiting value of 1 GPa is suggested for generic silicate materials.

IV. Methods

In this work, rather than assuming one consistent intrinsic tortuosity, pores filled below residual saturation instead lack hydraulic connectivity. That is, they do not contribute to permeability. Instead of integrating over all fluid filled pores, tortuosity is divided into two groups, those above and below residual. If those pores filled below residual saturation are hydraulically disconnected, these pores can be excluded from the summation or integration. Thus, rather than finding the mean squared hydraulic radius of all filled pores, it is only the mean squared radius of pores filled above residual saturation. That is:

$$\overline{r_c^2} = \frac{\gamma^2 \cos^2\theta}{S_w - S_r} \int_{S_r}^{S_w} \frac{dS'}{P_c^2} \tag{14}$$

With this rationale, the lower limit of integration on the Burdine relative permeability model is the residual saturation and relative permeability is unaffected by the capillary pressure extension below residual saturation, regardless of its magnitude.

$$k_{rw}^{Burdine} = X_{rw}^2 \frac{\int_{Sr}^{Sw} \frac{dS'_w}{P_c^2}}{\int_{Sr}^{1} \frac{dS'_w}{P_c^2}} \tag{15}$$

A similar concept was present in the original derivation of the Mualem relative permeability model[2]. Rather than weighting the squared hydraulic radius of the pore size distribution, Mualem proposed a model by weighing the supposed likelihood of two filled pores intersecting. Mualem initially declared a minimum pore radius upon which to perform the integration. That is, any pores of radius below this threshold would not contribute to the permeability. However, this lower pore radius limit was tacitly dropped when utilizing asymptotic capillary pressure models. That is, integration is generally assumed to be over all pores.

Here, by similarly grouping the pore connectivity into two groups, those below and above minimum pore radius, the residual saturation is the saturation at which the smallest pore to contribute to relative permeability is filled. At the same time, if there is a viable hydraulic pathway through the medium, the effective tortuosity must also be non-zero. Consequently, the Mualem model here is modified such that the lower limit of integration is the same residual saturation utilized in the effective tortuosity.

$$k_{rw}^{Mualem} = X_{rw}^{\eta} \left[\frac{\int_{r_{min}}^{r} \frac{dS'_w}{Pc}}{\int_{r_{min}}^{r_{max}} \frac{dS'_w}{Pc}} \right]^2 = X_{rw}^{\eta} \left[\frac{\int_{Sr}^{Sw} \frac{dS'_w}{Pc}}{\int_{Sr}^{1} \frac{dS'_w}{Pc}} \right]^2 \tag{16}$$

V. Case Study

Recent modifications to PFLOTRAN include several options for imposing smoothing of the capillary pressure and relative permeability functions below the residual water saturation of a porous medium up to a specified maximum capillary pressure value. While imparting more physical realism as described above, the following case study also

demonstrates how these changes can result in significant improvements to numerical solution search performance.

This case study was originally developed to study the potential thermal-hydrologic consequences associated with a hypothetical in-package criticality event related to the direct disposal of a dual-purpose canister (DPC) in a repository in an unsaturated alluvium host rock[34]. A single waste package is modeled in a half-symmetry domain where the repository sits at a depth of 250 m, above the water table, and a breach along the top of the package at 9,000 years after repository closure allows for meteoric water percolating through the medium to pool inside the package. The model geometry consists of a waste package with a square cross section measuring 1.67 x 1.67 m inside of an emplacement drift whose cross-section measures 4 x 4 m. Assuming equal, 40-m spacing of waste packages along the drift and equal 40-m spacing between drifts, the model domain uses symmetry to model half of a waste package and 20 m of the emplacement drift. All the physical properties of the model are described in Price et al.[34], but specific model characteristics such as geometry, permeability, and capillary pressure functions are described again in Figures 1 and 2.

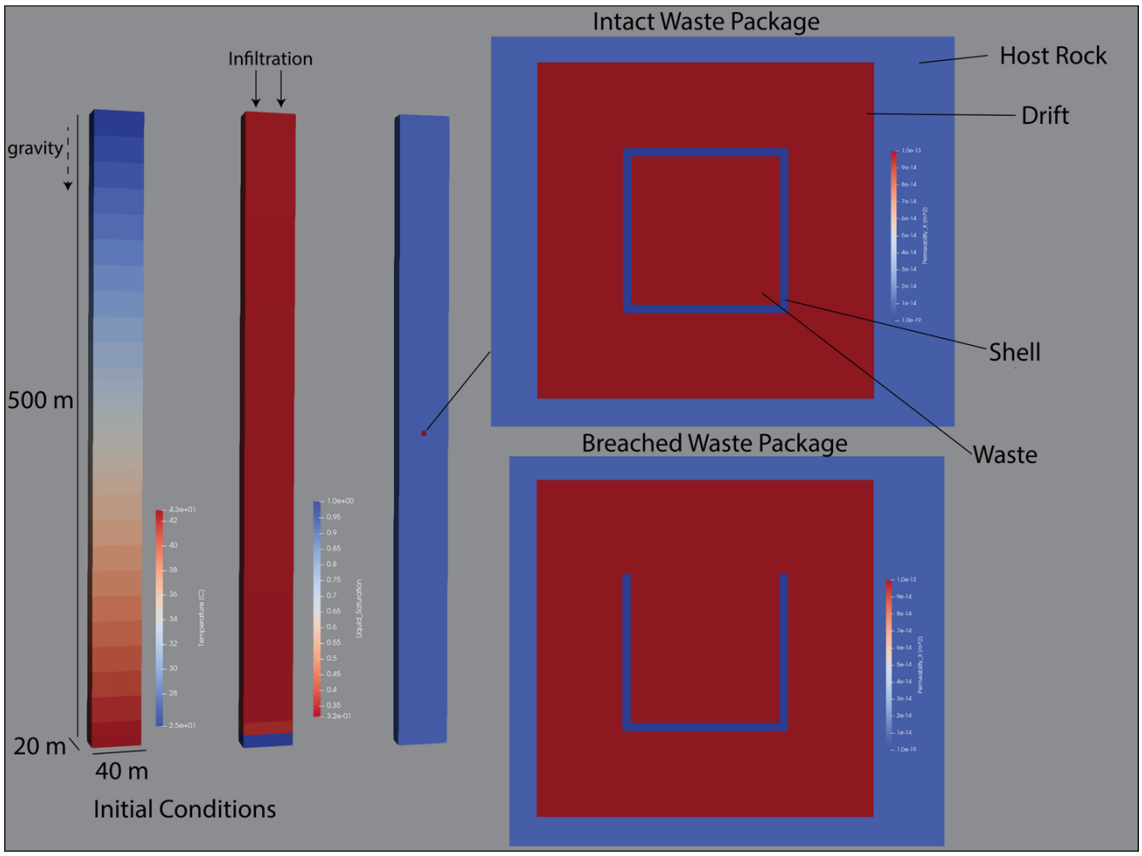

Figure 1: Model materials and setup. Left: initial temperature and saturation profile at repository closure. The rainfall infiltration boundary condition is applied along the top of the model in the direction of gravity. Right: Repository system colored by permeability.

In this conceptual model, a hypothetical critical configuration is achieved after 20,000 years by assuming engineered shielding mechanisms have failed at this point while the geometric configuration of the waste package internals remains. As a conservative assumption, the waste package is partially breached such that water (a neutron moderator) can enter the package and then pool at the bottom. At this point in time, thermal loading due to radioactive decay is past its peak, and the thermal effect of a hypothetical criticality event is added to the decay heat at a constant value. The goal of this study was to understand the maximum possible power level that could be sustained in such a situation. As a bounding assumption, the critical event can only be sustained so long as water remains in the waste package; therefore, this study sought to find the largest average

power level that could maintain liquid water in the waste package for different potential future infiltration rates over a repository performance period of 100,000 years. This approach was thought to be conservative since more realistically the waste would need to be submerged in liquid water to maintain a critical configuration.

Modeling this system inherently involves modeling capillary flow and evaporation of liquid water at and below the residual water saturation of the host rock. Previously, capillary pressure was modeled using the van Genuchten model truncated at a constant maximum value. To assess the effectiveness of the methods described earlier, the capillary pressure model is alternatively extended to a maximum of 0.1 GPa using an exponential interpolation. To ensure continuity and smoothness with an exponential extension to 0.1 GPa, the piecewise junction point occurs at $S_j = 0.1155$. Despite the very large difference in capillary pressure between the asymptotic and extended models below the junction, there are only minor differences in relative permeability as the effective tortuosity model dominates. Consequently, the closed-form analytic expressions of van Genuchten will be utilized here rather than implementing a complex piecewise but negligibly different relative permeability function in PFLOTRAN. The capillary pressure and relative permeability of the liquid phase in the conventional and revised models are plotted in Figure 2.

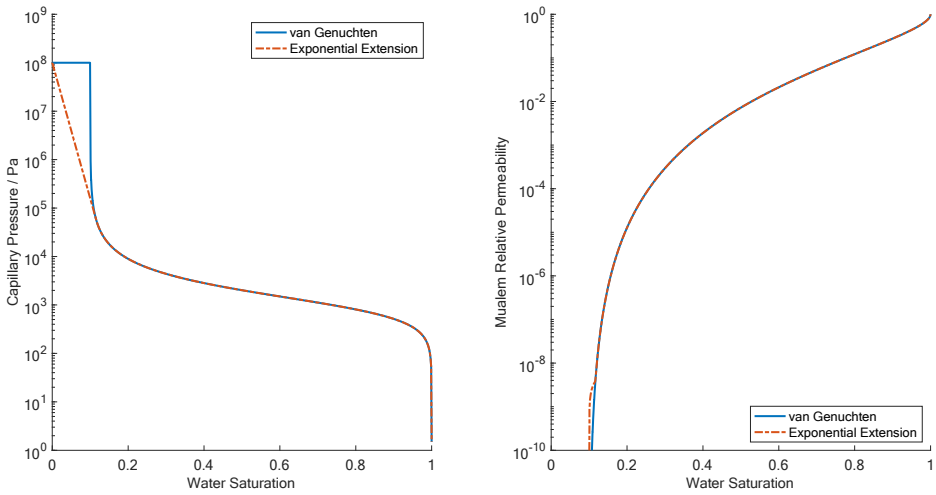

Figure 2: van Genuchten Capillary Pressure and Mualem Relative Permeability Models with an exponential extension to a maximum capillary pressure of 10^8 Pa. The van Genuchten parameters are $\alpha = 10^{-3}Pa$, $m = 0.5$, $n = 2$, and S_r=10%. The Mualem tortuosity exponent is $\eta = 0.5$. Because the piecewise junction occurs very near residual saturation (S_j= 0.1155), the difference in the derived relative permeability is negligible under the revised limits of integration.

As discussed previously, truncation of capillary pressure introduces a cusp into the capillary pressure function and can result in significant numerical challenges. Using the previous formulation for capillary pressure, this study encountered prohibitively slow runtimes, and simulations even failed to complete for some combinations of infiltration rate and criticality power level.

A comparison is presented here where a series of simulations is run for combinations of 2 infiltration rates both with and without a criticality event. These simulations are first run without capillary pressure function extensions, and then they are re-run with capillary pressure function extensions. For simplicity and ease of comparison, all materials in the domain were run with the same capillary pressure function.

The waste form internals are modeled as a homogeneous heat source distributed throughout the waste package in this study. A decay heat source corresponding to one half of a 37-PWR dual purpose canister (due to the symmetry assumption) is imposed on the model.[35] At 9,000 years the waste package is considered breached, and the top of the shell is removed (Figure 1). This causes the waste package to fill with meteoric water that has percolated downward through the domain. The presence of water in the waste package is required in this conceptual model for criticality to be able to occur. Then, at 20,000 years, a constant 100W fission power is added to the heat source for the remainder of the simulation where applicable (Figure 3) to simulate a criticality event. At the time of the criticality event, the fission power output constitutes a significant fraction of the thermal loading from the waste form.

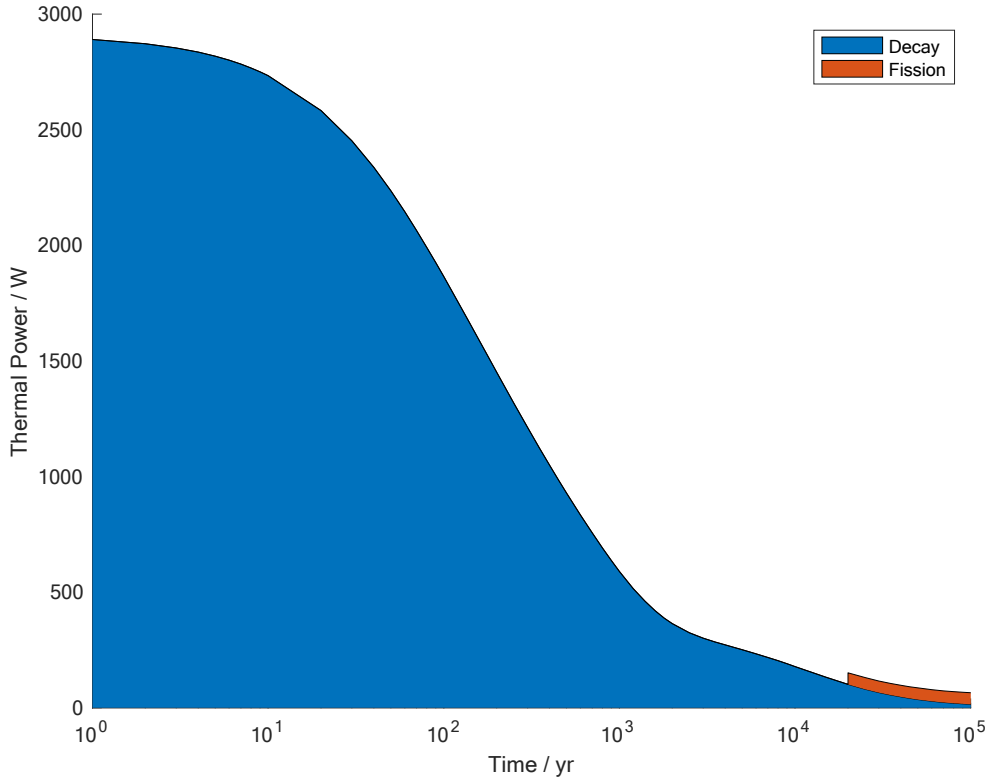

Figure 3: Power output from the waste form due to decay heat and the fission heat of a criticality event.

Boundary conditions on the sides of the domain impose zero heat and mass fluxes assuming symmetrical spacing of waste packages and drifts. The top of the domain consists of a Dirichlet temperature condition with a specified liquid flux and zero gas flux. Temperature is set to 25 C at the top, and liquid water infiltration from the top is modeled as either 2 mm/yr or 5 mm/yr depending on the modeled scenario. The bottom boundary is set to hydrostatic liquid pressure relative to a water table set at 10 m beyond the bottom of the domain, with an associated temperature of 43 C following a geothermal gradient and a dissolved air mole fraction of 1.0E-08 mol/mol. Models are run for a 2 mm/yr infiltration rate and 5 mm/yr infiltration rate with both 0W fission heat (only decay heat) and a 100W fission heat. This set is run with and without unsaturated capillary pressure function extensions resulting in a set of 8 distinct simulations. All models are run to 100,000 years.

VI. Results

Dry-out and Re-saturation

The 2 mm/year case with a 100W criticality event has been chosen to illustrate the impacts of using unsaturated capillary pressure extensions on dynamic dry out and re-saturation processes in 3D. In this model, there are two periods where dry-out and/or re-saturation with liquid water occur (Figure 4). The first period is in the very early time of the simulation, where a hot waste package is introduced into a partially saturated medium (Figure 1, intact waste package). The simulation is initialized with water saturations corresponding to an equilibrated water column everywhere, so water is initially present in the waste package cells. Within the first year after repository closure, the bottom of the waste package experiences dynamic changes in liquid saturation. Heating initially induces drying in the bottom cell, but – due to the low permeability of

the shell – convection drives water to pool and temporarily increases water saturations at the bottom of the waste package. This likely does not represent flow through a true (sealed) waste package at early time post-closure, but it does provide an excellent test case illustrating the numerical complexity of flow at low liquid saturation subject to a heat source.

Figure 4: Comparison of temperature and liquid saturation as a function of time in the bottom center cell of the waste package for the 2mm/yr infiltration rate case with a criticality event.

In the first year, simulations with and without capillary pressure extensions produce slightly different liquid saturation results in the bottom center cell, even though liquid saturations in this particular cell are above the residual saturation. The reason for this difference has to do with the fact that other neighboring cells *do* contain liquid saturations below the residual to varying degrees. This affects capillary pressures of the neighboring cells differently between the extended and unextended capillary pressure models and therefore creates slightly different flow pathways. A 2D snapshot and 1D transect of liquid saturations at 0.1 years through the waste package show subtle

differences in liquid saturations between 0 and the residual saturation (0.1), which then result in slightly different liquid fluxes to all cells in the vicinity of the waste package.

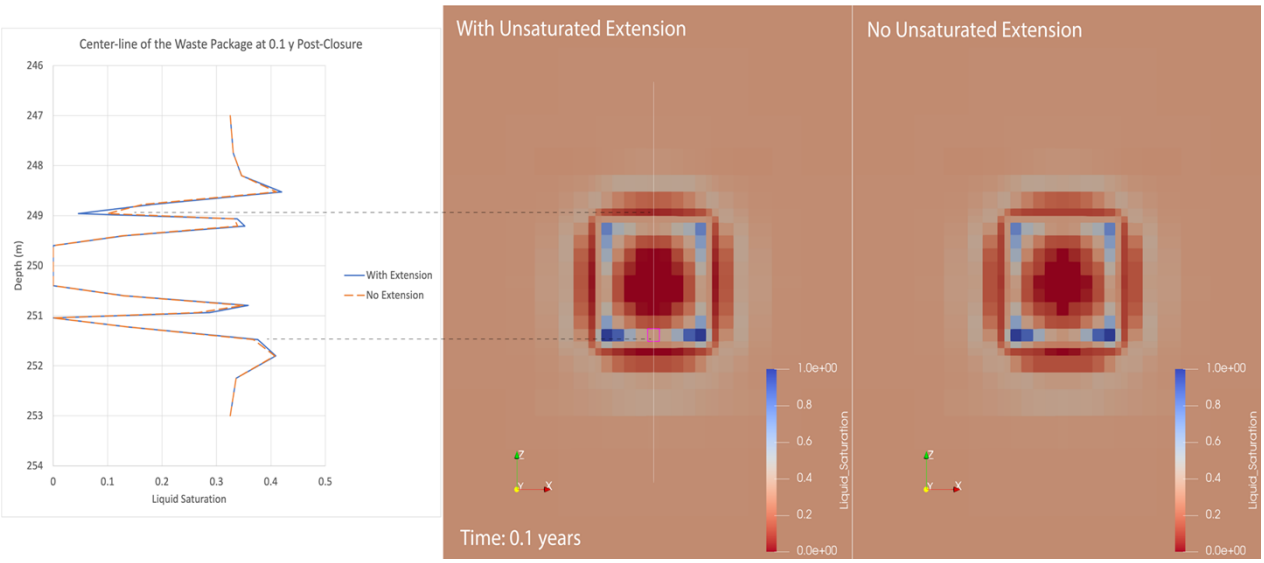

Figure 5: Liquid saturation for the 2mm/yr infiltration case 0.1 years after repository closure with and without unsaturated capillary pressure extensions, with a plot of liquid saturation along the centerline for both cases (left). The pink box denotes the location of the cell plotted in Figures 4 and 6.

The second dry-out and re-saturation phase occurs when the decay heat no longer provides enough power to keep the waste package completely dry, at around 14,000 years, and then with the introduction of the criticality event, at 20,000 years. The simulations with and without capillary pressure extensions both produce the same temperature profile and show similar trends in liquid saturation. As the decay heat drops, water begins to pool in the waste package, and liquid saturations increase. Then, when the fission heat is applied at 20,000 years, water is driven off again and the whole waste package begins to dry out. Full dry-out is not achieved even though the 100W fission power remains on for the rest of the simulation; the 100W fission power alone is not sufficient to drive all of the water away without enough additional decay heat. The extended and un-extended models do show slightly different patterns of re-saturation in

the period where decay heat is dropping and before the criticality event (Figure 6). This difference is more significant than the early-time fluctuations, likely because all cells in the waste package are re-saturating from being completely air-saturated. Ultimately at late time, both representations approach the same liquid saturations and temperatures.

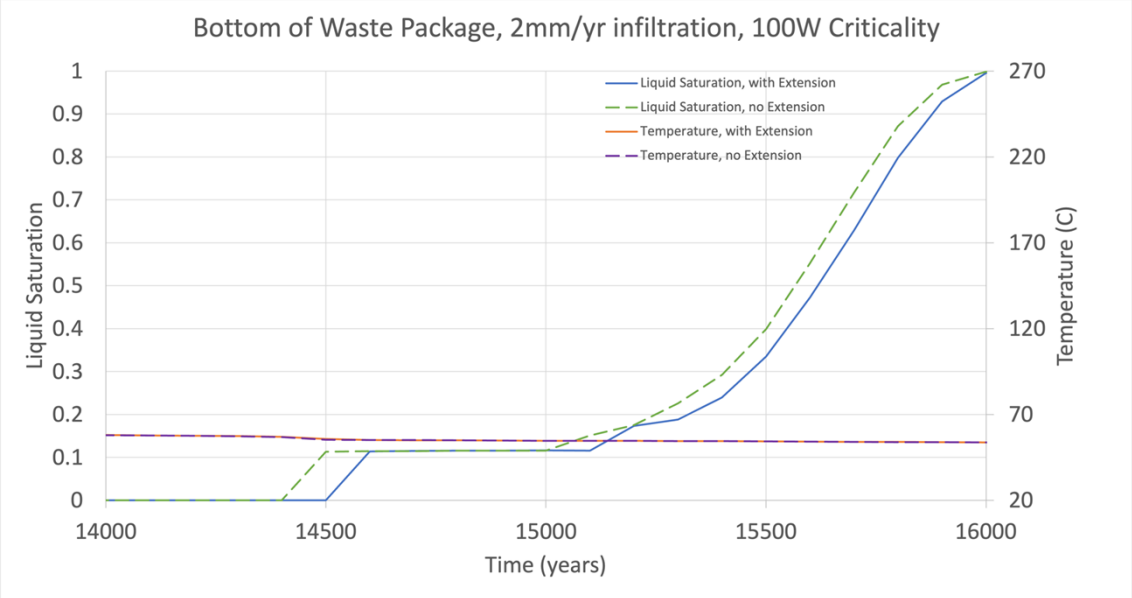

Figure 6: Comparison of re-saturation behavior after 14,000 years

Late-Time

The models are all run to 100,000 years; all models reach a steady state by this time. When a 100W criticality event is introduced in the model from 20,000 years to 100,000 years, the steady-state water level in the waste package depends on the infiltration rate (Figure 7). This reflects a balance between infiltration and evaporation for a constant 100W power input.

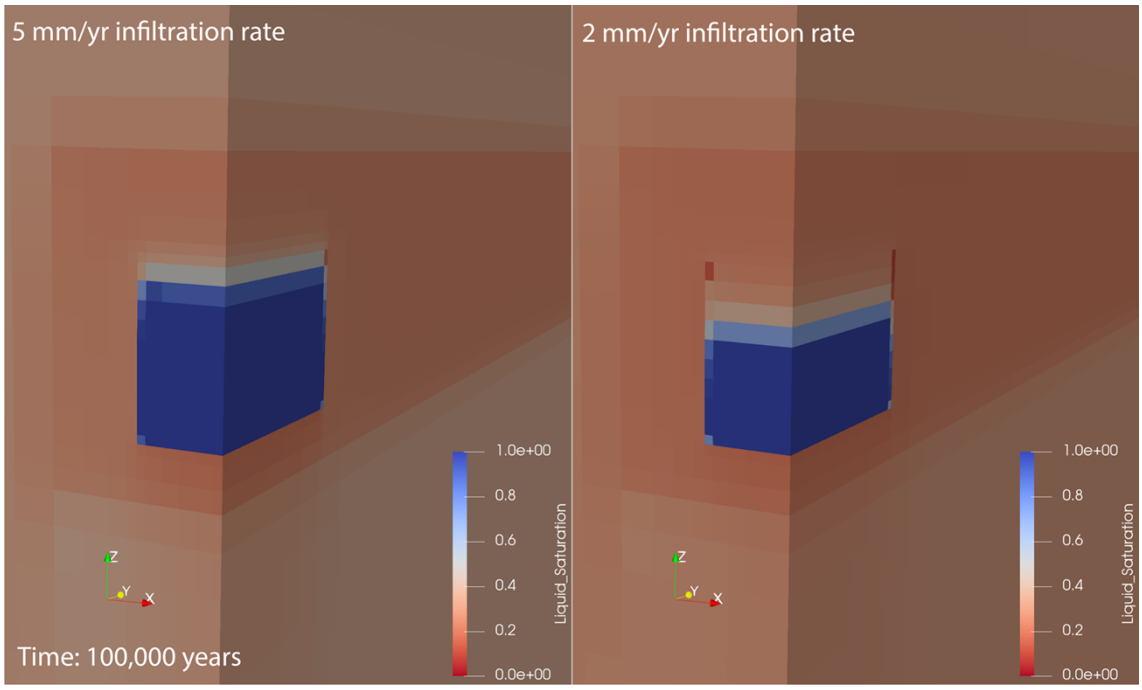

Figure 7: Steady-state water levels in the waste package during a 100W criticality event for a) a 5 mm/yr infiltration rate and b) a 2 mm/year infiltration rate.

Each of these simulations were run using a capillary pressure curve truncated at $1x10^8$ Pa and then run again with smooth exponential capillary pressure interpolation to the same max capillary pressure of $1x10^8$ Pa. The end results of the simulations were nearly identical (Figure 8), while the number of time steps and iterations necessary to complete the simulation reported in Table 1 and Table 2 show vastly different performance.

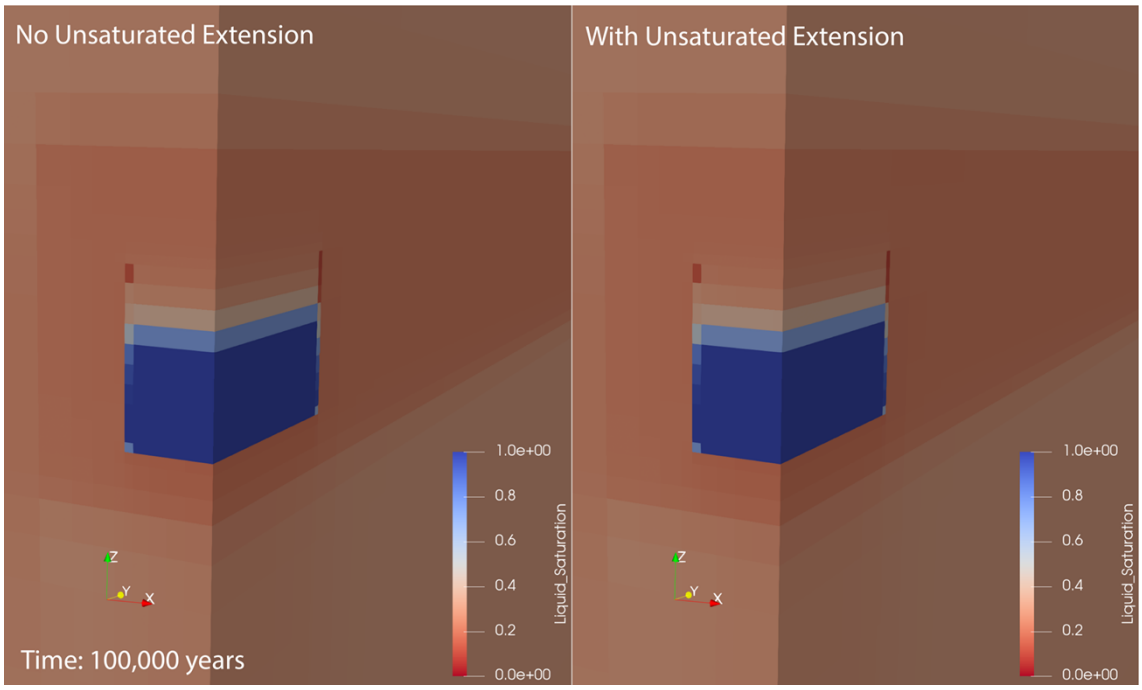

Figure 8: Steady-state water levels for the 2mm/year case with a 100W fission power level, with and without using unsaturated capillary pressure extensions.

Table 1: Flow Steps and Time Step Cuts with and without Unsaturated Extensions (UE) for each combination of infiltration rate and fission power level

Infiltration Rate (mm/yr)	**Fission Power (W)**	**Flow Steps**		**Time Step Cuts**	
		Without UE	With UE	Without UE	With UE
2	0	289,177	17,093	72,933	3,541
2	100	296,285	21,535	75,068	4,899
5	0	295,822	18,582	77,879	1,740
5	100	302,356	17,085	78,940	1,846

Table 2: Newton Iterations and Linear Iterations with and without Unsaturated Extensions (UE) for each combination of infiltration rate and fission power level

Infiltration Rate (mm/yr)	**Fission Power (W)**	**Newton Iterations**		**Linear Iterations**	
		Without UE	With UE	Without UE	With UE

2	0	916,827	66,365	66,462,018	8,288,274
2	100	945,627	86,401	68,171,896	9,488,116
5	0	954,945	52,073	65,594,716	8,047,312
5	100	978,773	50,258	67,208,891	7,276,634

VII. Discussion

Consistent with the findings of *Sun et al*.,[11] providing a smooth extension to the conventional concept of capillary pressure eliminates the instability in Newton's method. Here, each flow step involves computationally intensive steps like computation of the Jacobian as well as a series of nonlinear and linear iterations. On average, simulations that did not use smooth capillary pressure function extensions took 14 to 18 times more flow steps than those that did use capillary pressure function extensions for two otherwise identical simulations (

Table 1). Within a given flow step, the number of Newton iterations reflects how well the nonlinear solution search method is converging on a solution. Running without unsaturated extensions resulted in 11 to 20 times more total nonlinear iterations (Table 2); on average, Newton iterations per flow step is roughly the same between extended (3.4 iterations/flow step) and un-extended (3.2 iterations/flow step) scenarios. Interestingly, the average number of linear iterations per Newton iteration is higher with unsaturated extensions (133.5) than without (70.5). This generally reflects the conditioning of the Jacobian matrix, and the difference is probably due to the simulations using capillary pressure extensions taking fewer, and therefore larger, time steps. Model runtime varies with computer architecture, among other things; with an average decrease in number of flow steps by 15x for a constant number of Newton iterations per flow step, expected speedup when using capillary pressure function extensions for this problem would be roughly in line with change in number of flow steps (about an order of magnitude).

While the matric potential represents intermolecular chemical energy, the matric potential was not coupled to the overall energy balance. Above residual saturation, this energy is typically negligible compared with sensible heat or the latent heat of vaporization for water. However, this same assumption may not be valid below residual saturation where very large matric potentials are found. For example, the latent heat of vaporization for water between 0 and 100 C ranges between 2500.9 kJ/kg and 2256.54 kJ/kg. In comparison, a matric potential of 1 GPa under the assumption of incompressibility represents an additional 1000 kJ/kg. Consequently, the net energy required to remove water by evaporative processes can be significantly greater than expected from bulk properties estimates. Conversely, this excess heat of wetting is observable as sensible heat if the material is later re-wetted through imbibition or condensation. If implemented, this effect has the potential to dampen fluctuations in the temperature as it would dampen the change in sensible heat. Similarly, the ability to accurately model the matric potential in this regime is necessary to accurately model vapor pressure reduction, as per the Kelvin equation. This work enables residual saturation to be modeled independent of capillary pressure, enabling more accurate representations of humidity in a repository environment below residual saturation. In these simulations here, a more modest value of 0.1 GPa was simulated, where the matric potential is minor compared to the modeled sensible and latent heats. Thus, direct comparison of the results of the extended and truncated capillary pressure curves is justifiable.

VIII. Conclusions

In this work, the destabilizing effect of a singularity at residual saturation in conventional capillary pressure models was discussed. Using a hypothetical high-level nuclear repository as a test case, a significant performance improvement was demonstrated using a smooth and continuous exponential piecewise extension to the capillary pressure. That

is, both the number of linear and nonlinear iterations necessary to complete the simulation was reduced to less than one-tenth of truncated capillary pressure approach. This results in a commensurate reduction in computational resources necessary to complete a simulation where the instability at residual saturation is encountered.

While relative permeability is derived from capillary pressure data, here it was demonstrated that the relative permeability is largely insensitive to capillary pressure below residual saturation. That is, by modeling residual saturation as an effect of tortuosity, the relative permeability of the liquid water phase approaches zero at the residual primary due to a loss of hydraulic connectivity rather than excessive matric potential. Additionally, by treating the residual fluid as primarily disconnected pores and adsorbed films, for which there is no connectivity, the calculated relative permeability is justifiably indifferent to the modeled matric potential of the residual fluid.

Finally, a physical basis for limiting the capillary pressure was discussed. Relating capillary pressure to the matric potential and heats of adsorption, the maximum capillary pressure on silicate materials is, under the assumption of incompressibility, 1 GPa. However, as this energy is comparable to the heat of vaporization, future improvements to integrate the matric potential into the energy balance may have to be considered to accurately model this energy. In addition to thermal considerations, as this quantity is related to the degree of vapor pressure lowering, the matric potential is an important factor in calculating the humidity in a waste repository environment.

Acknowledgements

This article has been authored by an employee of National Technology & Engineering Solutions of Sandia, LLC under Contract No. DE-NA0003525 with the U.S. Department of Energy (DOE). The employee owns all right, title and interest in and to

the article and is solely responsible for its contents. This article was co-authored by staff from UT-Battelle, LLC under Contract No. DE-AC05-00OR22725 with the U.S. Department of Energy The United States Government retains and the publisher, by accepting the article for publication, acknowledges that the United States Government retains a non-exclusive, paid-up, irrevocable, world-wide license to publish or reproduce the published form of this article or allow others to do so, for United States Government purposes. The DOE will provide public access to these results of federally sponsored research in accordance with the DOE Public Access Plan https://www.energy.gov/downloads/doe-public-access-plan.

References

[1] M. T. OFOEGBU et al., “Geomechanical and Thermal Effects of Moisture Flow at the Proposed Yucca Mountain Nuclear Waste Repository,” *Nuclear Technology*, **134**, 3, 241 (2001); doi: https://doi.org/10.13182/NT01-A3199.

[2] K. W. CHANG, T. LAFORCE, and L. L. PRICE, “Hydro-thermal impacts on near-field flow and transport in a shale-hosted nuclear waste repository," *Tunnelling and Underground Space Technology,* **130**, 104765 (2022)); doi: https://doi.org/10.1016/j.tust.2022.104765.

[3] M. T. VAN GENUCHTEN, "A Closed-form Equation for Predicting the Hydraulic Conductivity of Unsaturated Soils," *Soil Science Society of America Journal*, **44**, 5, 892 (1980); doi: https://doi.org/10.2136/sssaj1980.03615995004400050002x.

[4] Y. MUALEM, "A new model for predicting the hydraulic conductivity of unsaturated porous media," *Water Resources Research*, **12**, 3, 513 (1976); doi: https://doi.org/10.1029/WR012i003p00513.

[5] Y. Y. W. TSANG, ”Yucca Mountain Heater Tests” in *Gas Transport in Porous Media*, Vol. 20, Part 3, Chap. 23, p. 371, Springer, Dordrecht, Netherlands (2006); doi: https://doi.org/10.1007/1-4020-3962-X_23

[6] M. NOLE *et al*., “GDSA PFLOTRAN Development (FY2021)," SAND2021-8709R, Sandia National Laboratories (July 2021); doi: https://doi.org/10.2172/1817333.

[7] S. SEVOUGIAN et al., "GDSA Repository Systems Analysis FY19 Update," SAND2019-11942R, Sandia National Laboratories (Oct. 2019); doi: https://doi.org/10.2172/1569793

[8] S. W. WEBB et al., "Thermally induced natural convection effects in Yucca Mountain drifts," *Journal of Contaminant Hydrology*, **62-63**, 713 (2003); doi: https://doi.org/10.1016/S0169-7722(02)00180-8.

[9] J. CHEN, J. W. HOPMANS, and M. E. GRISMER, "Parameter estimation of two-fluid capillary pressure–saturation and permeability functions," *Advances in Water Resources*, **22**, 5, 479 (1999); doi: https://doi.org/10.1016/S0309-1708(98)00025-6.

[10] H. D. PARK et al., "Newton trust-region methods with primary variable switching for simulating high temperature multiphase porous media flow," *Advances in Water Resources*, **168**, 104285 (2022); doi: https://doi.org/10.1016/j.advwatres.2022.104285.

[11] Y. SUN et al., "Modeling Thermal-Hydrologic Processes for a Heated Fractured Rock System: Impact of a Capillary-Pressure Maximum," *Transport in Porous Media*, **83**, 3, 501 (2010); doi: https://doi.org/10.1007/s11242-009-9459-1.

[12] M. MUSKAT and M. W. MERES, "The Flow of Heterogeneous Fluids Through Porous Media," *Physics*, **7**, 9, 346 (1936); doi: https://doi.org/10.1063/1.1745403.

[13] J. J. NITAO and J. BEAR, "Potentials and Their Role in Transport in Porous Media," *Water Resources Research*, **32**, 2, 225 (1996); doi: https://doi.org/10.1029/95WR02715.

[14] F. A. L. DULLIEN, F. S. Y. LAI, and I. F. MACDONALD, "Hydraulic continuity of residual wetting phase in porous media," *Journal of Colloid and Interface Science*, **109**, 1, 201-218 (1986); doi: https://doi.org/10.1016/0021-9797(86)90295-X.

[15] L. A. RICHARDS, "CAPILLARY CONDUCTION OF LIQUIDS THROUGH

POROUS MEDIUMS," *Physics*, **1**, 5, 318 (1931); doi: https://doi.org/10.1063/1.1745010.

[16] T. K. TOKUNAGA and J. WAN, "Water film flow along fracture surfaces of porous rock," *Water Resources Research*, **33**, 6, 1287 (1997); doi: https://doi.org/10.1029/97WR00473.

[17] M. C. LEVERETT, "Capillary Behavior in Porous Solids," *Transactions of the AIME*, **142**, 1, 152 (1941); doi: https://doi.org/10.2118/941152-g.

[18] J. BEAR, *Dynamics of Fluids in Porous Media*. Dover, New York, NY (1988).

[19] R. H. BROOKS and A.T. COREY, "Hydraulic Properties of Porous Media," in "Hydrology Papers," Colorado State University, Fort Collins, CO (1964).

[20] H. D. PARK et al., "Linear and nonlinear solvers for simulating multiphase flow within large-scale engineered subsurface systems," *Advances in Water Resources*, **156**, 104029 (2021); doi: https://doi.org/10.1016/j.advwatres.2021.104029.

[21] C. ROSSI and J. R. NIMMO, "Modeling of soil water retention from saturation to oven dryness," *Water Resources Research*, **30**, 3, 701 (1994); doi: https://doi.org/10.1029/93WR03238.

[22] S. W. WEBB, "A simple extension of two-phase characteristic curves to include the dry region," *Water Resources Research*, **36**, 6, 1425 (2000); doi: https://doi.org/10.1029/2000WR900057.

[23] J. NIESSNER, S. BERG, and S. M. HASSANIZADEH, "Comparison of Two-Phase Darcy's Law with a Thermodynamically Consistent Approach," *Transport in Porous Media*, **88**, 1, 133 (2011); doi: https://doi.org/10.1007/s11242-011-9730-0.

[24] N. T. BURDINE, L. S. GOURNAY, and P. P. REICHERTZ, "Pore Size Distribution of Petroleum Reservoir Rocks," *Journal of Petroleum Technology*, **2**, 7, 195 (1950); doi: https://doi.org/10.2118/950195-g.

[25] N. T. BURDINE, "Relative Permeability Calculations From Pore Size Distribution Data," *Journal of Petroleum Technology*, **5**, 3, 71 (1953), doi: https://doi.org/10.2118/225-g.

[26] N. E. EDLEFSEN and A. B. ANDERSON, "Thermodynamics of soil moisture," *Hilgardia*, **15**, 2, 31 (1943), doi: https://doi.org/10.3733/hilg.v15n02p031.

[27] J. R. PHILIP, "Unitary approach to capillary condensation and adsorption," *The Journal of Chemical Physics*, **66**, 11, 5069 (1977); doi: 10.1063/1.433814.

[28] M. TULLER, D. OR, and L. M. DUDLEY, "Adsorption and capillary condensation in porous media: Liquid retention and interfacial configurations in angular pores," *Water Resources Research*, **35**, 7, 1949 (1999); doi: https://doi.org/10.1029/1999WR900098.

[29] B. V. DERJAGUIN and N. V. CHURAEV, "Polymolecular adsorption and capillary condensation in narrow slit pores," *Progress in Surface Science*, **40**, 1, 173 (1992); doi: https://doi.org/10.1016/0079-6816(92)90045-J.

[30] C. ZHANG and N. LU, "What Is the Range of Soil Water Density? Critical Reviews With a Unified Model," *Reviews of Geophysics*, **56**, 3, 532 (2018); doi: https://doi.org/10.1029/2018RG000597.

[31] C. ZHANG, Y. DONG, and Z. LIU, "Lowest matric potential in quartz: Metadynamics evidence," *Geophysical Research Letters*, **44**, 4, 1706 (2017); doi:

https://doi.org/10.1002/2016GL071928.

[32] G. S. CAMPBELL and S. SHIOZAWA, "Prediction of Hydraulic Properties of Soils Using Particle-Size Distribution and Bulk Density Data," presented at the International Workshop on Indirect Methods for Estimating the Hydraulic Properties of Unsaturated Soils, Riverside, CA, Oct. 11-13, 1989, p. 317, University of California Press (1992).

[33] A. KHALFI and P. BLANCHART, "Desorption of water during the drying of clay minerals. Enthalpy and entropy variation," *Ceramics International*, **25**, 5, 409 (1999); doi: https://doi.org/10.1016/S0272-8842(98)00050-9.

[34] L. L. PRICE et al., “Preliminary Analysis of Postclosure DPC Criticality Consequences,” SAND2020-4106, Sandia National Laboratories (Dec. 2020); doi: https://doi.org/10.2172/1616378.

[35] S. PAINTER, et al., "ORNL Input to GDSA Repository Systems Analysis FY19," M4SF-190R010304072. Oak Ridge National Laboratory (2019).